

Discrete Particle Detection and Metal Emissions Monitoring Using Laser-Induced Breakdown Spectroscopy

D. W. HAHN,* W. L. FLOWER, and K. R. HENCKEN

Sandia National Laboratories, Livermore, California 94551-0969

The unique conditions for the application of laser-induced breakdown spectroscopy (LIBS) as a metal emissions monitoring technology have been discussed. Because of the discrete, particulate nature of effluent metals, the utilization of LIBS is considered in part as a statistical sampling problem involving the finite laser-induced plasma volume, as well as the concentration and size distribution of the target metal species. Particle sampling rates are evaluated and Monte Carlo simulations are presented for relevant LIBS parameters and wastestream conditions. For low metal effluent levels and submicrometer-sized particles, a LIBS-based technique may become sample limited. An approach based on random LIBS sampling and the conditional analysis of the resulting data is proposed as a means to enhance the LIBS sensitivity in actual wastestreams. Monte Carlo simulations and experimental results from a pyrolytic waste processing facility are presented, which demonstrate that a significant enhancement of LIBS performance, greater than an order of magnitude, may be realized by taking advantage of the discrete particulate nature of metals.

Index Headings: Laser-induced breakdown spectroscopy; Metal emissions monitoring; Particle detection.

INTRODUCTION

In recent years, considerable resources have been directed toward the development and testing of new continuous emissions monitors (CEMs) for metals in process wastestreams. The motivating factors that drive CEM development are diverse and include regulatory compliance, public assurance of treatment technologies, and process optimization and control. Recent draft maximum achievable control technology (MACT) standards encourage the development and use of continuous emissions monitors for metals.¹ One goal is the reduction or elimination of expensive compliance testing, thereby facilitating the permitting process. Furthermore, with waste treatment processes often coming under increased public scrutiny, continuous or near-continuous emissions data may be beneficial in promoting public confidence in treatment technologies.† An additional application that has gained attention is the use of CEM data for process control and optimization. Cost benefits can be realized by curtailing often expensive front-end waste characterization and by taking advantage of enhanced process efficiency via CEM data feedback. The broad scope of CEM incentives and potential benefits has led to a wide range of technologies and development efforts.

The technologies in the forefront of metals CEM de-

velopment include inductively coupled plasma atomic emission spectroscopy (ICP-AES), microwave-induced plasma atomic emission spectroscopy (MIP-AES), and laser-induced breakdown spectroscopy (LIBS), also referred to as laser-spark spectroscopy (LASS). A brief status report of these three technologies and their application as multi-metals CEMs was published recently.² The present paper will focus only on LIBS, the one technology of the three that has been demonstrated in the field as a real-time monitor that is both *in situ* and noninvasive. LIBS is an atomic emission spectroscopy diagnostic that utilizes a high-power pulsed laser beam as the excitation source. The resulting optical breakdown, also referred to as a laser-induced plasma or laser spark, excites all species within the probe volume, which then enables determination of elemental composition. The physical processes of LIBS have been investigated in previous studies, but generally, particulates smaller than about 10 μm are completely dissociated in the resulting plasma.^{3,4} The origin and uses of the LIBS technique have been summarized in several publications,^{5,6} and literature reviews of a wide range of LIBS studies have been published.⁷⁻⁹ The specific applications of LIBS for the analysis of aerosols,^{3,4,10-12} vapors,¹³ and combustion particulates¹⁴⁻¹⁶ include a number of metal species such as beryllium, lead, and mercury, coal particles, and metal hydrides. Nonetheless, while much progress has been made in understanding both the LIBS process and its particular application for metals sensing, important issues (e.g., lower detection limits) remain regarding its use as a metals CEM in thermal treatment processes.

The nature of the metal species in thermal treatment process effluent streams becomes a fundamental issue in the implementation of a LIBS-based CEM. Specifically, in waste combustion systems, the fate of metals is a complex phenomenon controlled by mechanisms such as particle entrainment, chemical interactions, vaporization, condensation, particle coagulation, and particle collection by air pollution control system (APCS) devices.^{17,18} Important parameters include the volatility of metal species and the treatment process temperature profile. As the combustion products cool downstream of the primary reactor, vaporized metals are expected to nucleate homogeneously or condense onto other particles. Homogeneous nucleation typically produces submicrometer-sized particles; heterogeneous condensation also favors enrichment of metals to the smallest particles due to their higher surface-area-to-mass ratios.¹⁷⁻²² Sodium, for example, was reported²³ to be enriched nearly completely in the submicrometer particle size range as a result of vaporization and subsequent nucleation/condensation during a pulverized coal combustion study. APCS devices such as

Received 2 January 1997; accepted 4 June 1997.

* Author to whom correspondence should be sent.

† A series of articles was published in 1997 in the Knoxville *News-Sentinel* detailing the call by community groups for installation of continuous emissions monitors on a Department of Energy incinerator operated in Oak Ridge, Tennessee.

venturi scrubbers, high-efficiency particulate air (HEPA) filters, and electrostatic precipitators (ESPs) are characterized by decreased collection efficiencies for submicrometer-sized particles.¹⁸ Although new devices offer improved collection efficiencies for submicrometer-sized particles, particulate metals in typical post-APCS wastestreams are most frequently of the submicrometer size. The resulting particulate emissions may include both homogeneous and multi-species metals, as well as metal-enriched fly ash. The successful coupling of the LIBS technology as a metals CEM must consider and make use of the discrete, particulate nature of most metal species under applicable wastestream outlet conditions.

The purpose of this paper is to address the unique application and process conditions of LIBS as a metal emissions monitoring technology. Because of the particulate nature of effluent metals, the utilization of LIBS may be considered in part as a statistical sampling problem involving the finite laser-induced plasma volume, the LIBS duty cycle, and the concentration and size distribution of the target metal species. Particle sampling rates are discussed, and Monte Carlo simulations are presented for relevant LIBS parameters and wastestream conditions. An approach based on random LIBS sampling and the conditional analysis of the resulting data is proposed as a means to enhance the LIBS sensitivity in actual wastestreams. Experimental results from a pyrolytic waste processing facility are presented that demonstrate the significant enhancement of LIBS performance realized by taking advantage of the discrete particulate nature of metals.

LIBS SAMPLING STATISTICS

The sampling statistics associated with a LIBS-based metals CEM may be defined in terms of the average metal effluent concentration, the size distribution of metal particles, the laser repetition rate, and the plasma/spark volume. When the average number of metal particles sampled by each laser pulse becomes less than unity, as discussed below, the following two issues become important: (1) How many particles must be sampled to determine an accurate particle representation?, and (2) Can accurate metal concentration values be determined in the limiting case of low particle loadings?

Particle Sampling Rates. The LIBS technique utilizes a pulsed laser to generate the plasma spark, with typical repetition rates of about 10 Hz or less. For a given flow streamline within a wastestream, the spatial sampling efficiency is defined by the bulk flue gas velocity, laser pulse rate, and laser spark dimensions. The actual volume of the laser spark is a complex function of laser beam geometry, laser pulse energy, and ambient conditions. For present calculations, the plasma volume will be approximated as $5 \times 10^{-5} \text{ cm}^3$, which corresponds to a diameter of several hundred micrometers and a length of several millimeters, with the resulting shape corresponding to a truncated cone, as reported by Radziemski et al.³ The plasma volume does expand following breakdown initiation, but the overall geometry remains similar. For a nominal gas velocity of 2 m/s and 10-Hz repetition rate, the spatial sampling efficiency of the LIBS probe oriented perpendicular to the duct flow is about 0.1%. This compares with a 100% sampling efficiency for isokinetic ex-

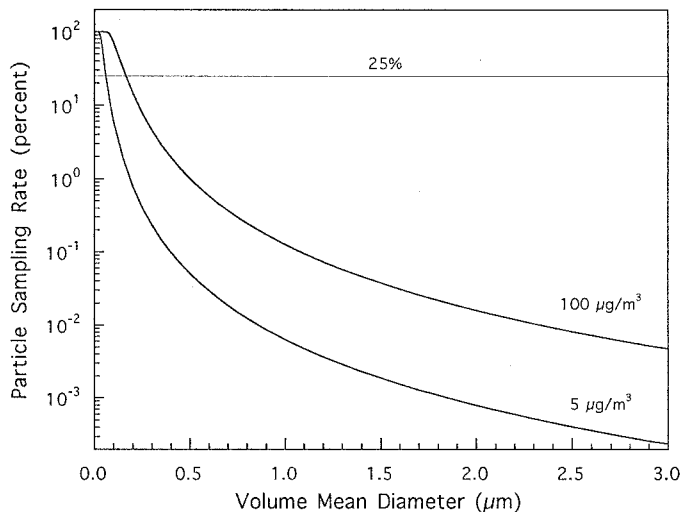


FIG. 1. Calculated LIBS particle sampling rates, expressed as percentage of shots sampling at least one particle, as a function of the volume mean diameter of a given particle size distribution.

tractive sampling along the corresponding streamline. The LIBS sampling efficiency may be increased by increasing the laser repetition rate, but consideration must be given to sample biases from pulse-to-pulse interactions, stemming, for example, from the LIBS-induced shock waves. A nominal LIBS spatial sampling efficiency on the order of 0.1% should not, however, be construed as limiting, because valid statistical representations are routinely constructed from much smaller sample spaces.

A fundamental parameter for LIBS sampling statistics may be defined as the particle sampling rate (PSR), which is equal to the percentage of laser pulses expected to sample at least one particle. Assuming a Poisson distribution function, the PSR is given by the expression

$$\text{PSR} = (1 - e^{-\mu}) \cdot 100 \quad (1)$$

where μ is the average number of particles per laser spark volume. For a given metal concentration x ($\mu\text{g}/\text{m}^3$), metal particle density ρ (g/cm^3), plasma volume V_{plasma} (cm^3), and particle volume mean diameter d_{VMD} (μm),

$$\mu = \frac{6xV_{\text{plasma}}}{\pi\rho d_{\text{VMD}}^3} \quad (2)$$

By making use of the volume mean diameter in the above equation, where

$$d_{\text{VMD}} = \left[\int_{d=0}^{\infty} d^3 p(d) dd \right]^{1/3} \quad (3)$$

one does not use any implicit particle distribution function $p(d)$ for Eq. 2. For a nominal plasma volume of $5 \times 10^{-5} \text{ cm}^3$, as discussed above, and a particle density value of $7.5 \text{ g}/\text{cm}^3$ [based on an average of the Resource Conservation and Recovery Act (RCRA) metals As, Be, Cd, Cr, Co, Mn, Ni, Pb, and Sb], particle sampling rates are presented in Fig. 1 as a function of volume mean diameter for the two concentration values of 5 and $100 \mu\text{g}/\text{m}^3$. We note that the cubic meter refers to an actual cubic meter (acm) and differs from the dry standard cubic meter (dscm) often used for emissions data. For a $100\text{-}\mu\text{g}/\text{m}^3$ concentration, the PSR is 25% for a volume mean

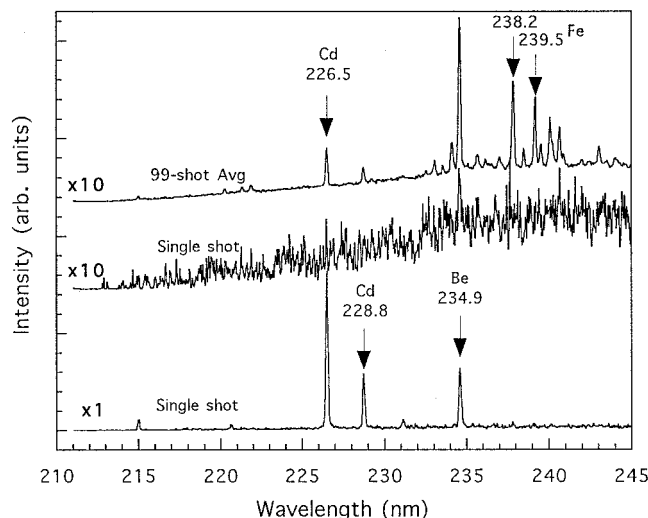


Fig. 2. Two single-shot spectra and 99-shot average spectrum for LIBS data collected from a rotary kiln incinerator wastestream. Spectra have been scaled as indicated, are presented with the same intensity units, and have been shifted vertically for clarity.

diameter of $0.175 \mu\text{m}$ and falls to below 1% for a d_{VMD} greater than $0.5 \mu\text{m}$. For the $5\text{-}\mu\text{g}/\text{m}^3$ concentration, which is typical of target metal effluent levels, the volume mean diameter must be $0.06 \mu\text{m}$ or smaller to reach a 25% PSR, with the PSR falling to 0.05% for a volume mean diameter of $0.5 \mu\text{m}$. For a PSR of 0.05%, an average of 2000 laser pulses would be required to sample a single target metal particle. The PSR results are based on an average metal density of $7.5 \text{ g}/\text{cm}^3$ and will scale inversely as the density is varied. For example, using the density of Be ($2 \text{ g}/\text{cm}^3$ and much lower than that of the other RCRA metals) will increase the calculated PSRs by a factor of about 3.7. In addition, effluent metals may also exist as oxides or salts, and the resulting densities will affect the sampling rates accordingly. Nonetheless, these calculations demonstrate that a large increase in sampling rate results from a larger number of small particles and, conversely, that the sampling rate can become exceedingly small for realistic combinations of particle size and metal concentration.

As an example of the discrete nature of metal particles in actual effluent wastestreams, a set of LIBS spectra is presented in Fig. 2. The data were recorded in the U.S. Environmental Protection Agency rotary kiln incinerator simulator (RKIS) facility at Research Triangle Park, North Carolina. The RKIS consists of a primary combustion chamber, a transition section, and a fired afterburner in the secondary combustion chamber. Both the kiln and afterburner were fitted with 73-kW auxiliary fuel burners and were fired with natural gas. The LIBS sampling port was located downstream from a heat exchanger section and diluent air injector. The flue gas temperature was constant at approximately $232 \text{ }^\circ\text{C}$ ($450 \text{ }^\circ\text{F}$) at the sample port for all LIBS sampling, and the water vapor content was approximately 7% mole fraction. Figure 2 contains the average spectrum of a 99-shot laser pulse sequence recorded at 6.5 Hz and two single-shot spectra from the same sequence. The recorded EPA Reference Method 29 concentration values were $195 \mu\text{g}/\text{acm}$ of cadmium and $225 \mu\text{g}/\text{acm}$ of beryllium. Moderate signals

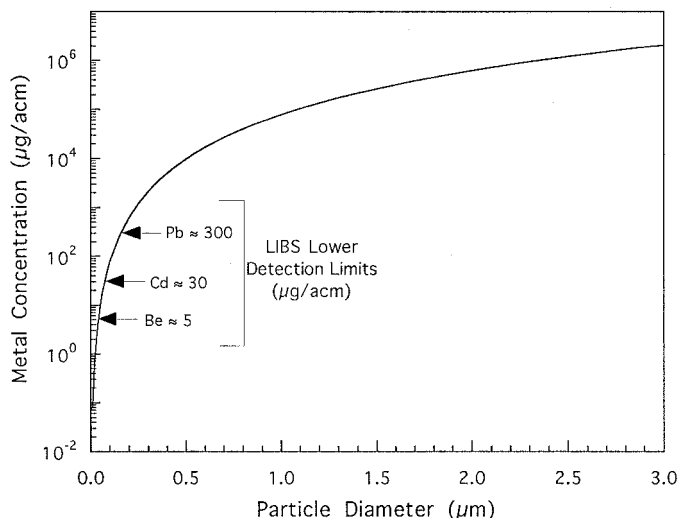


Fig. 3. Equivalent metal concentration for single particle hit as a function of particle diameter. Approximate LIBS lower detection limits of select species are indicated.

corresponding to Cd, Be, and Fe (from the fly ash) are visible in the averaged 99-shot spectrum. However, one of the single-shot spectrums contains only a trace of Be at 234.9 nm and no Cd or Fe features, while the second single-shot spectrum contains a Cd signal at 226.5 nm that saturated the detector. We note that detector saturation results in lost intensity signal and a corresponding reduction in calculated metal concentration. The equivalent single-shot cadmium concentration was approximately $3900 \mu\text{g}/\text{acm}$, about 20 times larger than the average cadmium concentration represented by the upper spectrum.

The data presented in Fig. 2 suggest a solution to the dilemma of low particle sampling rates that utilizes the discrete and often disparate LIBS single-shot signals. Specifically, the PSRs can become limiting when the averaging of a small number of particle hits with a very large number of total shots reduces the signal-to-noise ratio to below significant levels. However, as demonstrated in Fig. 2, single particle hits can contain disproportionately large signals for specific metals that could provide LIBS data under very low PSR conditions. By using a conditional analysis approach in which single-shot particle "hits" are separated from single-shot particle "misses", one may take advantage of the discrete particle signals in response to these potentially limiting sampling rates. As an example, the equivalent concentrations of a single particle based on the LIBS parameters outlined above are presented in Fig. 3 as a function of the single particle diameter. Also noted in Fig. 3 are the approximate LIBS lower detectability limits for a range of target metals. The calculations presented in Fig. 3 reveal that significant metal concentrations result from particles on the order of several hundred nanometers, and consequently, large single-shot LIBS signals are available. With the adoption of a single-shot detection and conditional analysis approach, the implementation of a LIBS-based metals CEM may be considered in the context of a statistical particle sampling problem.

Monte Carlo Simulations. The issues associated with the use of conditional signal analysis in conjunction with

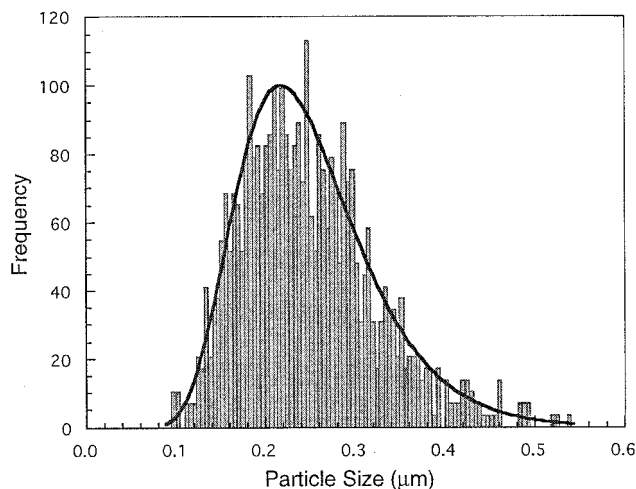


FIG. 4. Ideal ZOLD distribution (solid curve) for $\bar{d} = 0.25 \mu\text{m}$ and $\sigma_0 = 0.30$. The histogram represents 1000 random samples from the 3765-element particle set ($\bar{d} = 0.25 \mu\text{m}$ and $\sigma_0 = 0.30$) used for Monte Carlo calculations. The plots have been normalized by using the modal value.

the LIBS technique may be considered in two parts: (1) the necessary number of particle samples required to represent accurately the true particle size distribution; and (2) the necessary number of particle samples required to represent accurately the true particle loading or sampling frequency. Monte Carlo calculations were performed to address these two questions.

To examine the effects of discrete particle sampling from a size distribution of particles, we performed a series of calculations using as a model the zeroth-order logarithmic distribution (ZOLD) for particle size.²⁴ The general ZOLD, $p(d)$, is functionally similar to the log-normal distribution and is defined as

$$p(d) = \frac{\exp(-\sigma_0^2/2)}{\sigma_0 d_m \sqrt{2\pi}} \exp\left[-\frac{(\ln d/d_m)^2}{2\sigma_0^2}\right] \quad (4)$$

where d_m is the modal or most probable value, and σ_0 is a measure of the width and skewness of the distribution function. The ZOLD is normalized to unity over the integral range of zero to infinite and is skewed toward larger particle sizes, making it a good representation of nucleating and coagulating aerosols. The first and third moments of Eq. 4 define the mean and volume mean diameters (see Eq. 3), respectively, which after integration yield

$$\bar{d} = d_m \exp(1.5\sigma_0^2), \quad (5)$$

$$d_{\text{VMD}} = d_m \exp(2.5\sigma_0^2). \quad (6)$$

The ZOLD is presented in Fig. 4 for a mean diameter of $0.25 \mu\text{m}$ and a value of $\sigma_0 = 0.30$. $\sigma_0 = 0.30$ is the approximate value for the self-preserving size distribution for aerosol coagulation.^{25,26} For these parameters, the modal and volume mean diameters are $0.218 \mu\text{m}$ and $0.274 \mu\text{m}$, respectively. For Monte Carlo calculations, a particle set was constructed from the ZOLD distribution by limiting the probabilities of the largest and smallest diameters to 1% of the most probable value and partitioning the resulting diameter range into 100 intervals. For $\bar{d} = 0.25 \mu\text{m}$ and $\sigma_0 = 0.30$, the 1% probabilities occur at

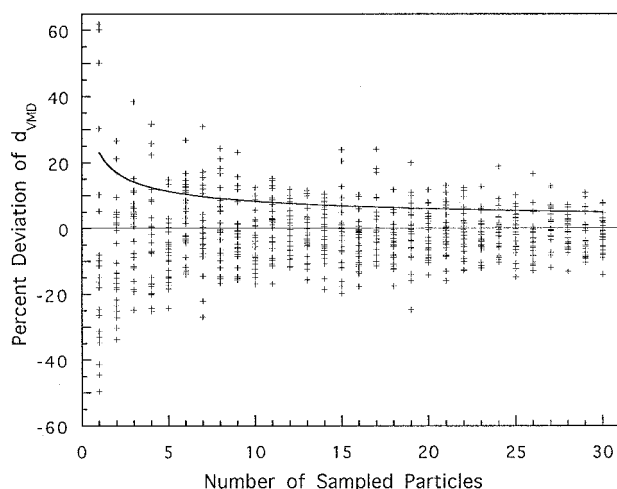


FIG. 5. Percent deviations of the calculated volume mean diameter as a function of the number of particles sampled. The parameters $\bar{d} = 0.25 \mu\text{m}$ and $\sigma_0 = 0.30$ were used for the particle distribution. Twenty-five Monte Carlo trials are presented for each sample number, and the solid curve represents the average (absolute value) of 250 trials for each sample number.

diameters of $0.087 \mu\text{m}$ and $0.543 \mu\text{m}$. By setting the number of particles at the modal value equal to 100, we constructed the corresponding particle set, which contained a total of 3765 particles. The mean and volume mean diameters of the 3765 particles were $0.249 \mu\text{m}$ and $0.271 \mu\text{m}$, respectively. The 3765 particle sizes were entered into a one-dimensional array that was then randomly accessed with the use of a pseudo-random number generator. In a procedure to assess the Monte Carlo algorithm, a series of histograms were generated from the particle set and compared to the ideal ZOLD function. The histogram of 1000 particles randomly accessed from the 3765-element array is presented along with the ideal ZOLD in Fig. 4. The mean and volume mean diameters of the 1000 particles are equal to $0.247 \mu\text{m}$ and $0.269 \mu\text{m}$, respectively. A series of trials produced excellent overall agreement with the ideal ZOLD values and provided a validation of the Monte Carlo algorithm.

With the use of the 3765-element particle set, a series of Monte Carlo trials were conducted to characterize the deviation of the volume mean diameter on the basis of a small, discrete number of samples in comparison to the total population value, namely, $0.271 \mu\text{m}$. The volume mean diameter was selected for comparison because a LIBS-based CEM requires particle mass information. Presented in Fig. 5 are the percent deviations of the calculated d_{VMD} values for each of 25 trials, as the number of averaged particle samples was varied from 1 to 30. Figure 5 also includes the average percent deviation (absolute value) for 250 trials of each corresponding sample size. What is noted in Fig. 5 is that, by about 20 sampled particles, the deviation of the volume mean diameter is limited to within 20% of the true value, while the average deviation is about 7.5%. A series of 500 trials was conducted for each sample size from 1 to 30, and it was found that, by 19 particle samples, 80% of the trials yielded a d_{VMD} within 10% of the expected value. Similar results were obtained for other size distribution widths and volume mean diameter values up to micrometer-

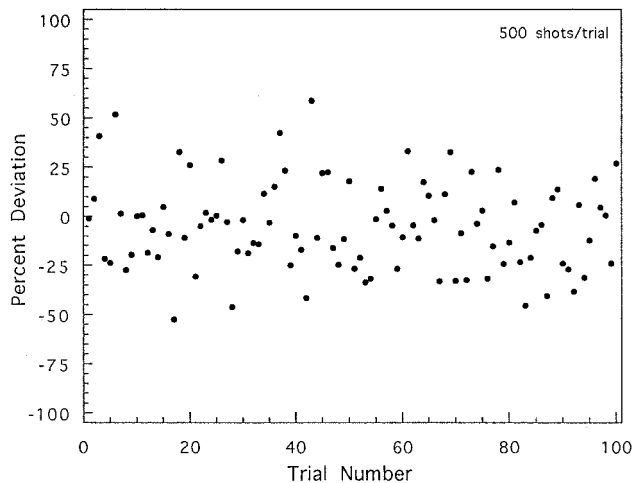


FIG. 6. Percent deviations of the calculated concentration based on 500 total shots presented for 100 individual Monte Carlo trials. The parameters $\bar{d} = 0.25 \mu\text{m}$, $\sigma_0 = 0.30$, and $100 \mu\text{g}/\text{m}^3$ were used for the particle distribution, and Eqs. 1 and 2 were used for particle sampling rates.

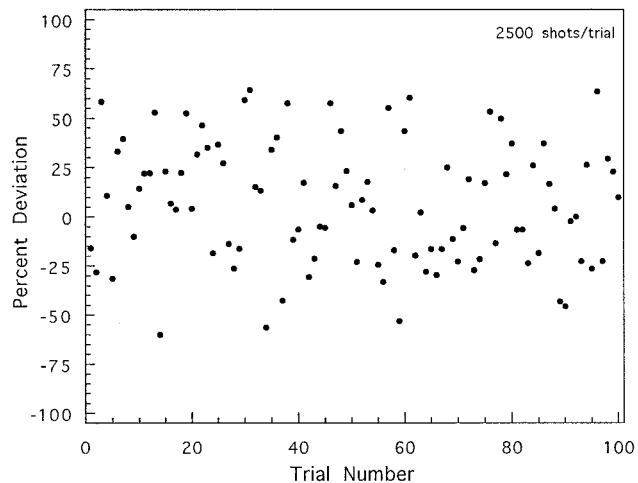


FIG. 7. Percent deviations of the calculated concentration based on 2500 total shots presented for 100 individual Monte Carlo trials. The parameters $\bar{d} = 0.25 \mu\text{m}$, $\sigma_0 = 0.30$, and $10 \mu\text{g}/\text{m}^3$ were used for the particle distribution, and Eqs. 1 and 2 were used for particle sampling rates.

sized. The Monte Carlo calculations demonstrate that only a small number of particles, approximately 20, are required to provide an accurate representation of the average particle mass for rather broad ranges of submicrometer to micrometer-sized simulated aerosol dispersions.

In addition to the measurement of an average particle mass, the successful implementation of a metals CEM necessitates the simultaneous determination of the particle number density or particle sampling frequency. Specifically, if the conditional analysis approach is used to segregate the particle hits from the particle misses, thus increasing signal-to-noise ratio and sensitivity, the actual metal concentration x may be determined from the relation

$$x = (\text{average metal concentration for hits}) \times (\text{sampling frequency of hits}) \quad (7)$$

where the average concentration of the hits is determined by using any standard LIBS calibration technique but utilizing only the spectra of hits, and the frequency of hits is the ratio of the number of hits to total laser shots. Therefore the overall metal concentration measurement is reduced to the product of two statistical samples, namely, the particle size distribution and the particle sampling frequency. Monte Carlo simulations were performed to assess the overall viability of the conditional analysis approach to a LIBS CEM.

For a specified metal concentration, mean particle diameter, and σ_0 value for the ZOLD, a particle distribution set was constructed as described above, and particle sampling probabilities were evaluated with the use of Eqs. 1 and 2. A binary system was used for the sampling probabilities, with the probability of hitting no particles (i.e., particle miss) equal to $\exp(-\mu)$ and the probability of hitting a single particle (i.e., particle hit) equal to $1 - \exp(-\mu)$. For the low PSR cases simulated, the probabilities of hitting two particles or more were several orders of magnitude lower than the single particle probability; therefore Eq. 1 was used as the probability of a single particle hit only. The Monte Carlo calculations were then performed for a specified number of total shots

by using the following algorithm: Each shot was classified as a hit or miss by randomly addressing the binary hit/miss probability distribution as defined above. For each shot classified as a miss, only the total shot count was incremented. For each shot classified as a hit, a particle size was then selected randomly and stored from the particle size distribution array, as in the above calculations, and both the total shot count and hit count were incremented. After the total number of desired shots, the average metal concentration was calculated by using the volume mean diameter for all particle hits, plasma volume, and frequency of hits, as defined by Eq. 7. The calculated average metal concentration was then compared to the specified (i.e., input) concentration value, and the percent deviation was calculated.

Figure 6 contains the percent deviations of the calculated metal concentrations of 100 Monte Carlo trials for the specified case of $100 \mu\text{g}/\text{m}^3$, $0.25\text{-}\mu\text{m}$ mean particle diameter, $\sigma_0 = 0.30$, and 500 total shots. The corresponding particle sampling rate is 6.0%, based on Eq. 1. The average percent deviation of the calculated concentrations for the 100 trials is 18.6% with a standard deviation of 13.5%. The average particle sampling rate was 6.11% with a standard deviation of 0.96%, and the average number of particle hits was 30.6 with a standard deviation of 4.8. For these trials, typically the number of sampled particles was greater than the minimum of 20, as discussed above, and the resulting combination of mean volume and sampling frequency produced very good agreement with the specified concentration value.

Figure 7 contains the percent deviations of the calculated metal concentrations of 100 Monte Carlo trials for the same conditions as Fig. 6, but with a specified concentration of $10 \mu\text{g}/\text{m}^3$, and for 2500 total shots per trial. The corresponding predicted particle sampling rate is 0.62%. The average percent deviation of the calculated concentrations for the 100 trials is 26.3% with a standard deviation of 17.0%. The average particle sampling rate was 0.68% with a standard deviation of 0.14%, and the average number of particle hits was 16.9 with a standard

deviation of 3.6. For these sampling rates, the nominal concentration of the averaged hits was about $1400 \mu\text{g}/\text{m}^3$, as compared to the overall value of $10 \mu\text{g}/\text{m}^3$, which demonstrates the potential for increased signal-to-noise ratios. For these trials, the typical number of sampled particles was less than the prescribed value of 20, and the spread was somewhat larger in comparison to the Fig. 6 data. Nonetheless, the Monte Carlo results are encouraging in that reasonable accuracy (26% average) was obtained for the calculated concentration values under simulated conditions that would severely limit a conventional LIBS approach.

One more consideration is noted with regard to the above calculations and data analysis approach, and it concerns the total number of shots. To obtain a valid measure of the frequency of particle hits, one should terminate the conditional analysis algorithm on the basis of the total number of shots rather than a selected total number of hits. This requirement may be explained by using the example of a six-sided die with equal probabilities for all sides. To determine the probability of a given number (i.e., side) using the total number of *hits* concept, one would record the true probability of 1/6th only when the desired side was observed on exactly the sixth toss. In contrast, if the desired side was observed on the first toss, an incorrect value of 100% (i.e., 1 hit for one toss) would be determined. The inclusion of all possible outcomes (such as 50% for a hit after two shots, etc.) demonstrates the limited chance of recording the true probability. Alternatively, with the total number of *shots* approach, the likelihood of recording the true probability is much higher. Consider, for example, a total of six shots, where the desired side should occur on average once in every six tosses, which significantly increases the likelihood of obtaining the true probability. Analogous statistics hold for a conditional analysis approach to a LIBS CEM that could result in an inadvertent source of error, especially for the case of low particle sampling rates, if one is using a total number of hits approach.

EXPERIMENTAL

In a procedure to assess the above sampling statistics calculations and the conditional analysis approach, actual LIBS data were collected and evaluated in real time from a thermal treatment process wastestream. All data were recorded at a natural-gas-fired, pilot-scale, pyrolytic waste processing unit. The 220-kW burner was partially fired for this series of tests, and the pyrolytic processing chamber was operated at a temperature of 870°C (1600°F) under nonoxidizing conditions. The gaseous exhaust stream from the pyrolytic chamber entered a direct-fired secondary combustion chamber, then passed through a waste heat recovery unit, and finally passed through a wet gas scrubber before exiting the stack. Because of the relatively low operating temperatures of the primary pyrolytic unit, nearly all metal components of the waste feed were removed in a separate, solid-waste exit stream. The resulting metal concentrations in the stack effluent gas stream have been historically low, from tens of parts per billion (ppb) to sub-ppb levels.

The data presented here were recorded for a waste feed stream of 21 lb/h of municipal solid waste. The LIBS

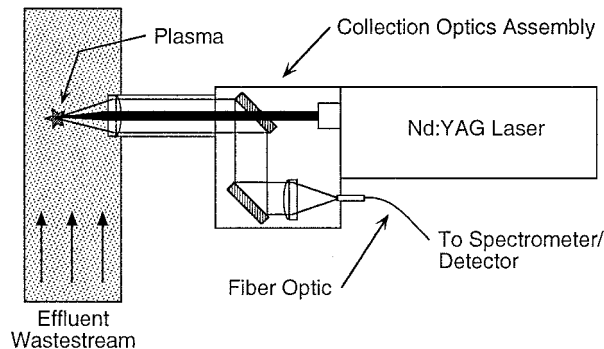


FIG. 8. Schematic diagram of the LIBS metals emissions monitor as installed on a process wastestream.

excitation source was a 1064-nm Nd:YAG laser with a nominal pulse width of 10 ns and pulse energy of 300 mJ. The laser beam was expanded to 12 mm and then focused to create the plasma by using a 75-mm-focal-length, 50-mm-diameter UV-grade quartz lens. The 50-mm lens also functioned to collect the plasma and atomic emission. A schematic diagram of the LIBS system is presented in Fig. 8. LIBS spectra were collected at 5 Hz with the use of a spectrometer and time-gated charge-coupled device (CCD) array. The CCD intensifier gate width was $3.5 \mu\text{s}$, with a time delay of $6.0 \mu\text{s}$ from the laser pulse. We used 1000-shot laser pulse sequences, during which individual shots were analyzed in real time for the presence of a given metal analyte. After each 1000-shot laser pulse sequence, the metal concentrations were calculated by using a laboratory calibration scheme based on integrated analyte peak intensity normalized by the continuum plasma emission. True metal concentrations were calculated on the basis of the average spectra of identified metal hits only, multiplied by the frequency of hits, as expressed in Eq. 7. The data were collected within a 2-h reference method (RM) sampling interval that utilized extractive sampling and analytical techniques in accordance with the EPA draft Method 29 standards. The LIBS sample port was located 35 in. downstream from the Method 29 sample port.

Chromium, manganese, and iron signals were measured consistently during the test cycle by using the conditional data analysis approach. The typical LIBS "hit" rates realized in the process stack were about 2%. For a sampling rate of 2%, to first order, the resulting signal-to-noise ratio is improved by a factor of 50 with the conditional analysis approach in comparison to an ensemble average. Representative spectra are presented in Figs. 9 and 10 corresponding to the subset of hits for iron and manganese, respectively, along with the 1000-shot ensemble-averaged spectra. The significant increase in analyte signal is apparent in the two figures, demonstrating the advantage of the conditional data analysis approach for LIBS-based metals monitoring.

Metal concentration values were sequentially logged throughout the 2-h reference method for the metal analytes of interest, namely, iron and the Clean Air Act metals chromium and manganese. The current prototype system operated in a single-species detection mode and was therefore cycled through the target species. Representative concentration data recorded for manganese are pre-

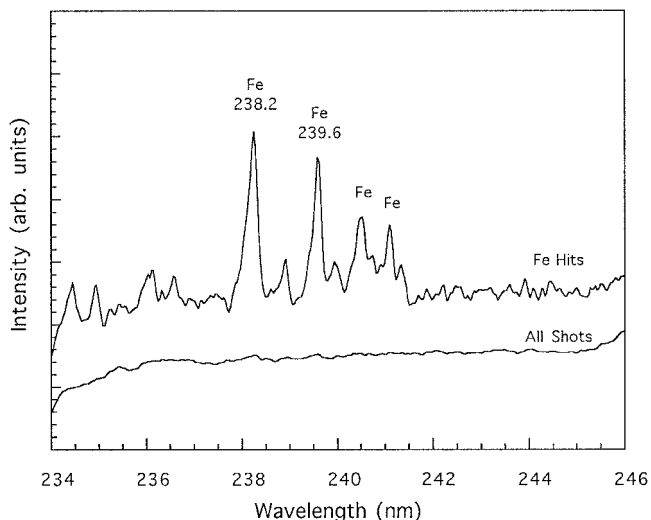


Fig. 9. The 1000-shot average spectrum and the average spectrum for identified iron hits for LIBS data collected from a pyrolytic waste processor effluent stream. The recorded EPA Reference Method 29 iron concentration was 39.9 $\mu\text{g}/\text{acm}$. Spectra are presented with the same intensity scale units and have been shifted vertically for clarity.

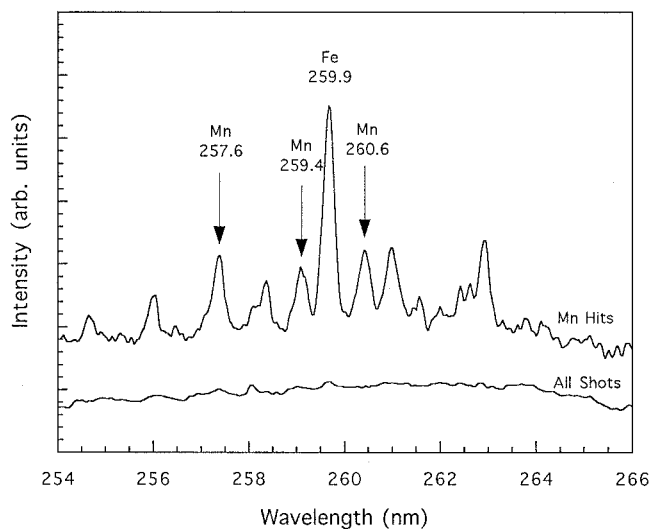


Fig. 10. The 1000-shot average spectrum and the average spectrum for identified manganese hits for LIBS data collected from a pyrolytic waste processor effluent stream. The recorded EPA Reference Method 29 manganese concentration was 3.3 $\mu\text{g}/\text{acm}$. Spectra are presented with the same intensity scale units and have been shifted vertically for clarity.

sented in Fig. 11. We note that the reported concentration unit of $\mu\text{g}/\text{acm}$ is approximately equal to a part per billion on a mass basis. Also included in Fig. 11 is the 2-h average value reported for the Method 29 extractive sampling. The average manganese concentration for the LIBS data of Fig. 11 is 3.3 $\mu\text{g}/\text{acm}$, and is in exact agreement with the Method 29 value of 3.3 $\mu\text{g}/\text{acm}$. Chromium was measured at a concentration of 2 to 3 $\mu\text{g}/\text{acm}$ and was consistently 21% lower than the Method 29 values. Iron was measured at concentrations from 40 to 140 $\mu\text{g}/\text{acm}$ and was consistently 36% lower than the Method 29 values.

As mentioned above, the particle sampling rates were typically 2% and ranged from about 1 to 4%. For the 1000-shot laser pulse sequences utilized, these rates correspond to a total number of particle hits on the order of 20, which is consistent with the necessary number of samples as discussed with respect to the Monte Carlo calculations. Overall, the experimental data are in excellent agreement with the numerical simulation results and demonstrate the quantitative application of the LIBS technique to an actual process wastestream with ppb-level metal effluent concentrations.

DISCUSSION

The important issue of metal particle sampling with a LIBS-based effluent monitoring system has been elucidated with the above calculations and LIBS field data. From our present analysis, the following two observations can be made: (1) the discrete nature of metal particulates in effluent waste streams can potentially be a limiting factor in LIBS monitoring, and (2) appropriate conditional data analysis schemes can greatly enhance the sensitivity and applicability of a LIBS metals monitor. The latter point is significant, because while LIBS offers the advantage of noninvasive, *in situ* monitoring, the overall LIBS sensitivities to targeted RCRA metals lag somewhat behind those of more mature technologies such as ICP-AES. However, the unique single-shot data gen-

erated with the LIBS technique contain information that may be exploited to expand the detectability range for effluent monitoring.

Our calculations demonstrate that for submicrometer-sized metal particle distributions and for effluent levels of about 10 $\mu\text{g}/\text{acm}$ (typical of many treatment process wastestreams), LIBS particle sampling rates may fall to 1% or less. Under conditions of such low sampling rates, simple time averaging of spectral data may or may not be sufficient for signal analysis. However, analysis of individual spectra from an effluent wastestream has revealed the disparate nature of metal LIBS data. We have shown that single-shot spectra may contain metal signals 20 times greater than the multishot-averaged metal signals. Because higher spectral signal levels offer increased

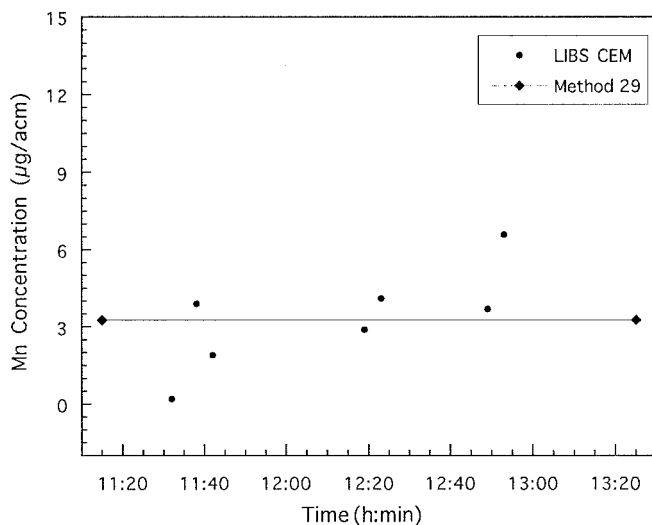


Fig. 11. LIBS manganese concentration data recorded as a function of time in a pyrolytic waste processor effluent stream. The LIBS data represent individual 3-min samples. The solid line is the EPA Reference Method 29 manganese concentration value reported for the 2-h sample period.

signal-to-noise ratios, working with the discrete LIBS spectra is desirable. Working with a select subset of LIBS-generated data, however, presents several statistical sampling problems. These issues were evaluated by using Monte Carlo simulations. It was determined that the number of particles required to accurately characterize the volume mean diameter or mass loading of rather broad particle distributions was not great, approximately 20 particles. Hence, characterization of mass loadings may be determined for low particle sampling rates ($\approx 1\%$) with sampling periods of 2–3 min for a reasonable sampling rate (< 10 Hz). These numbers are consistent with real-time emissions monitoring requirements and are compatible with our prototype LIBS monitoring system parameters.

Another issue associated with the segregation of discrete particle hits is the determination of overall effluent concentration levels from the subset of LIBS data. Consideration must be given to the overall data sampling process, with emphasis on the introduction of potential sample bias. Any method of *a priori* particle detection, such as light scattering or optical breakdown thresholding (i.e., breakdown triggered by a particle), may lead to significant biasing with regard to both particle size and particle composition. The conditional analysis approach that we discuss avoids these problems by sampling at a fixed laser repetition rate—thus achieving a uniform, random sample. Actual effluent concentration levels would be determined from the combination of the sampling frequency and the concentration of the spectral data for target particle hits only. This approach was demonstrated by using Monte Carlo simulations for representative effluent concentration levels and particle size distributions. Our calculations demonstrated that the conditional analysis approach yields accurate concentration values while significantly increasing the signal-to-noise ratios of the spectral data. Assessment of a conditional analysis routine by using data collected from an actual waste processing effluent stream provided very encouraging results. Specifically, wastestream concentrations of chromium, manganese, and iron were determined, which were in very good agreement with Method 29 reference data at levels that were significantly lower (factor of 30) than our established minimum detectable concentrations for a simple time-averaging mode. The resulting particle sampling rates were on the order of several percent—values consistent with our Monte Carlo calculations.

In addition to the use of LIBS data for metals concentration monitoring, further spectral information is available. Specifically, single-shot spectra contain information about the distribution of particulate mass loadings and the partitioning and correlation of metal species. As a research tool, for example, the analysis of individual spectra may provide insight into the partitioning of metal species onto fly ash particulates. Such information may be useful for the design of APCS or for air pollution dispersion models. A statistical approach could be used to determine the correlation of shot-to-shot signals between different metal species and with ash constituents (i.e., Si and Fe). The amount of information potentially available from the LIBS technique makes it a unique candidate for metals effluent monitoring.

CONCLUSION

A continuous emissions monitor for metals offers several potential benefits to end-users, including the possible curtailment of expensive front-end waste characterization and allowing the selection of operational strategies that maximize efficiency. The specific advantage of the LIBS technique is that it can measure total metals embedded in particles or in liquid aerosols, which account for most of the metals emitted from hazardous waste treatment processes, in a real-time, non-invasive manner. The technological approach of LIBS as a metals CEM has been verified, but the key issue of instrument response to *actual* wastestream conditions remains. In this paper we have addressed the issues associated with the discrete nature of many metal effluents in the context of particle sampling statistics. A Monte Carlo approach has been used to assess the utility of a proposed conditional data analysis technique. The numerical simulations and experimental data demonstrate that significant increases in the LIBS signal-to-noise ratio are attainable by using a statistical approach. The overall sensitivity and applicability of the LIBS technique as a metals CEM may in fact be defined on a case-by-case basis as determined by particular wastestream characteristics. Fine tuning the overall instrument to specific conditions may lead to enhanced sensitivity and performance.

ACKNOWLEDGMENTS

This work was supported in part by the U.S. Department of Energy, Office of Technology Development, Characterization, Monitoring, and Sensors Technology Crosscutting Program (CMST-CP), and the U.S. Department of Defense, Office of Munitions, Joint Services Demil Technology Office. We would like to acknowledge Shapoor Hamid and Jerry Holt of Balboa Pacific Corporation for providing access to their facility and for their assistance with the field test. We gratefully acknowledge the technical assistance of Howard Johnsen, Edward Walsh, and Lawrence Peng of Sandia. D.W.H. would like to acknowledge Stephan Weeks and Bill Haas of CMST-CP Field Support for useful technical discussions. W.L.F. would like to acknowledge C. J. DeCarli for helpful discussions during the early stages of this research.

1. U.S. Environmental Protection Agency, Draft Technical Support Document for HWC MACT Standards, Volume III, Selection of proposed MACT Standards and Technologies (February 1996).
2. N. B. French and M. Durham, Proc. International Conf. on Incineration and Thermal Treatment Technologies (1996), p. 399.
3. L. J. Radziemski, T. R. Loree, D. A. Cremers, and N. M. Hoffman, *Anal Chem.* **55**, 1246 (1983).
4. S. Yalcin, D. R. Crosley, G. P. Smith, and G. W. Faris, *Haz. Waste Haz. Mater.* **13**, 51 (1996).
5. K. Laqua, "Analytical Spectroscopy Using Laser Atomizers", in *Analytical Laser Spectroscopy*, N. Omenetto, Ed. (Wiley, New York, 1979), Chap. 2.
6. D. A. Cremers and L. J. Radziemski, "Laser Plasmas for Chemical Analysis", in *Laser Spectroscopy and Its Applications*, L. J. Radziemski, R. W. Solarz, and J. A. Paisner, Eds. (Marcel Dekker, New York, 1987), Chap. 5.
7. *Laser-Induced Plasmas and Applications*, L. J. Radziemski and D. A. Cremers, Eds. (Marcel Dekker, New York, 1989).
8. L. J. Radziemski, *Microchemical J.* **50**, 218 (1994).
9. S. A. Darke and J. F. Tyson, *J. Anal. At. Spectrom.* **8**, 145 (1993).
10. R. W. Schmieder, *Techniques and Applications of Laser Spark Spectroscopy*, Sandia National Laboratories Report SAND83-8618 (Sandia National Laboratory, Livermore, California, 1983).
11. L. J. Radziemski and T. R. Loree, *J. Plasma Chem. Plasma Proc.* **1**, 281 (1981).

12. J. P. Singh, H. Zhang, F. Y. Yueh, and K. P. Carney, *Appl. Spectrosc.* **50**, 764 (1996).
13. C. Lazzari, M. DeRosa, S. Rastelli, A. Ciucci, V. Pallechi, and A. Salvetti, *Laser and Particle Beams* **12**, 525 (1994).
14. D. K. Otteson, J. C. F. Wang, and L. J. Radziemski, *Appl. Spectrosc.* **43**, 967 (1989).
15. W. L. Flower, L. W. Peng, N. B. French, H. A. Johnsen, and D. K. Otteson, Proc. International Incineration Conf. (1994), p. 73.
16. H. Zhang, J. P. Singh, F. Y. Yueh, and R. L. Cook, *Appl. Spectrosc.* **49**, 1617 (1995).
17. R. G. Barton, W. E. Clark, and W. R. Seeker, *Combust. Sci. and Tech.* **74**, 327 (1990).
18. W. P. Linak and J. O. L. Wendt, *Prog. Energy Combust. Sci.* **19**, 145 (1993).
19. S. K. Friedlander, *Smoke, Dust and Haze* (John Wiley and Sons, New York, 1997).
20. W. P. Linak, R. K. Srivastava, and J. O. L. Wendt, *Combust. Sci. Tech.* **101**, 7 (1994).
21. W. P. Linak and J. O. L. Wendt, *Fuel Processing Tech.* **39**, 173 (1994).
22. R. G. Rizeq, D. W. Hansell, and W. R. Seeker, *Fuel Processing Tech.* **39**, 219 (1994).
23. N. B. Gallagher, L. E. Bool, J. O. L. Wendt, and T. W. Peterson, *Combust. Sci. and Tech.* **74**, 211 (1990).
24. W. F. Espenscheid, M. Kerker, and E. Matijevic, *J. Phys. Chem.* **68**, 3093 (1964).
25. S. C. Graham and A. Robinson, *J. Aerosol Sci.* **7**, 261 (1976).
26. K. W. Lee, *J. Colloid Interface Sci.* **92**, 315 (1983).